Available online at www.sciencedirect.com

ScienceDirect

www.elsevier.com/locate/jes

JES JOURNAL OF ENVIRONMENTAL SCIENCES

www.jesc.ac.cn

Application of an aerosol electrical mobility spectrum analyzer: Charged-particle polarity ratio measurement in the Antarctic and Arctic regions

Handol Lee[1], *Hyeok Chung*[2], *Kang-Ho Ahn*[3,*]

[1] *Department of Environmental Engineering, Inha University, 100 Inha-ro, Michuhol-gu, Incheon 22212, South Korea*
[2] *Aerosol Research and Technology Plus (ART+), 195-62, Daepyeong-ro, Daewol-myeon, Icheon, Gyunggi-do 17343, South Korea*
[3] *Department of Mechanical Engineering, Hanyang University, ERICA, 55 Hanyangdaehak-ro, Sangnok-gu, Ansan 15588, South Korea*

ARTICLE INFO

Article history:
Received 20 August 2020
Revised 23 December 2020
Accepted 23 December 2020

Keywords:
Aerosol electrical mobility spectrum analyzer
Antarctic
Arctic
Charged-particle polarity ratio

ABSTRACT

An aerosol electrical mobility spectrum analyzer (AEMSA), developed at Hanyang University, was employed to investigate the particle charge characteristics in the Antarctic and Arctic regions. The particle charge characteristics in these areas were compared with the charging state in Ansan, South Korea, located in the midlatitude, where artificial factors, such as human activity, urbanization, and traffic, might result in a higher total concentration. Furthermore, in Ansan, South Korea, the charged-particle polarity ratio was very stable and was close to 1. However, notably different particle charge characteristics were obtained in the Antarctic and Arctic regions. The imbalance between the numbers of positively and negatively charged particles was evident, resulting in more positive charges on the atmospheric particles. On average, the positively charged particle concentrations in the Antarctic and Arctic areas were 1.4 and 2.8 times higher, respectively, compared with the negatively charged particles. The developed AEMSA system and the findings of this study provide useful information on the characteristics of atmospheric aerosols in the Antarctic and Arctic regions and can be further utilized to study particle formation mechanisms.

Introduction

Aerosol particles are emitted from various sources, such as deserts, oceans, and industrial emissions, and they are widely distributed in the atmosphere through atmospheric transport, evaporation, and convection (Chu et al., 2016; Dallósto et al., 2017; Han et al., 2008; Jokinen et al., 2018; Kumar and Guleria, 2017; Liu et al., 2020). It is widely known that the properties of atmospheric particles, including size, concentration, morphology, and composition, are critical parameters in determining the local and global climate by engaging in scattering and absorption of solar radiation and cloud formation

* Corresponding author.
E-mail: khahn@hanyang.ac.kr (K.-H. Ahn).

https://doi.org/10.1016/j.jes.2020.12.028

(Carslaw et al., 2002; Charlson et al., 1992; Hansen et al., 1997; He et al., 2019; Li et al., 2020). Therefore, particle characterization techniques have been developed over time to estimate these properties of the atmospheric particles: impactor (inertia), cyclone (inertia), electrical mobility analyzer (electrical mobility), optical particle counter (scattering), aerodynamic particle sizer (inertia), balancing (mass), diffusion battery (diffusivity), and electron microscopy. The details of these aerosol measurement instruments are well represented in the work by McMurry (2000). These advanced techniques have led to important discoveries concerning atmospheric aerosol physics and chemistry as a connection to the effects of aerosols on atmospheric environments.

Another important parameter of atmospheric particles that significantly influences climate change patterns is the charging state of particles, i.e., the number of charged particles and their polarities. Since Raes and Janssens (1985) showed experimental evidence of the connection between ions and nucleation mechanisms, the importance of ions and charged particles in the atmosphere has been attracting considerable attention. Atmospheric particles are charged through various mechanisms, such as thunderstorms, electrified shower clouds, and cosmic ray ionization, and charged particles accelerate cloud formation owing to the enhanced condensation rate of molecules with polarity (Rycroft et al., 2007; Saunders, 1992; Snow-Kropla et al., 2011; Usoskin and Kovaltsov, 2006; Yu and Turco, 2001). Harrison (2004) highlighted that a profound understanding of atmospheric electrical systems, combined with cloud microphysics and cosmic rays, would offer important insights into climate science. The effects of particle charging state on particle behaviors in the atmosphere under specific conditions have also been investigated. Gilbert et al. (1991) measured electrical charges of ash particles to study deposition mechanisms of aggregated volcanic-ash particles, and Harrison et al. (2010) discussed the possibilities of charging mechanisms for volcanic-ash particles. Nicoll et al. (2011) investigated charging mechanisms of atmospheric particles in the elevated Saharan dust layers and the effects of charge on particle motion and collection. They additionally mentioned that a clear explanation of the observed results might become available with particle polarization measurement. In another interesting study, performed by Renard et al. (2013) using a balloon flight equipped with stratospheric and tropospheric aerosol counters, charged particles were observed at an altitude below 10 km in the troposphere and above 20 km in the stratosphere. However, uncharged particles were observed between these altitudes. The aforementioned studies focused primarily on the charging rate of the atmospheric particles, largely neglecting their polarities.

In a previous study, an aerosol electrical mobility spectrum analyzer (AEMSA) was developed that consists of a saturator, condenser, mobility analyzer, and detector — laser and charge-coupled device (CCD) camera. The AEMSA detects the electrical mobility spectrum and polarity of nanometer-sized charged particles. The performance of the AEMSA was demonstrated by measuring the equilibrium charging state of monodisperse particles (Ahn and Chung, 2010), and the AEMSA was successfully employed to analyze the particle charge polarity during a lightening event (Lee and Ahn, 2017). In this research, the AEMSA was utilized for monitoring the charging state of the atmospheric particles in the Antarctic and Arctic regions, where different particle-charging characteristics are expected because of prominent features of these areas, including the absence of the human activity and urban environments and different annual cycles of solar radiation compared with the midlatitudes. The AEMSA can be employed in various applications and areas for investigating the effects of charged particles in the atmosphere.

1. Method

1.1. *Instrument*

The AEMSA was utilized for investigating aerosol charging phenomena for atmospheric particles. A schematic diagram of the AEMSA is shown in Appendix A Fig. S1a. The AEMSA resembles a combination of a differential mobility analyzer (DMA) and a condensation particle counter. It employs a fixed electrical potential between two parallel electrodes to differentiate particles based on their electrical mobilities. The distance between the two electrodes is 9 mm, and the length of the electrodes is 50 mm. A total aerosol flow of 0.4 L/min is sampled through the inlet of the AEMSA, and 0.012 L/min is extracted and passes through the capillary tube. The remainder of the flow passes through a filter and a saturator (35°C), where isopropyl alcohol (IPA) evaporates and is transformed into a particle-free saturated IPA vapor flow. Particles injected from the capillary tube are carried by the saturated vapor flow, following which the supersaturated IPA vapor condenses onto the particles to form larger droplets at a condenser part maintained at 10°C, which can be easily detected by an optical detector.

Based on the principle of the AEMSA, neutral particles, i.e., zero charge, are detected at the middle of the analyzed region, and charged particles migrate because of the electrical force and are detected at certain detection locations, depending on particle electrical mobility and charge polarity. Fig. S1b shows a typical example of the data obtained by the AEMSA for ambient particles. Smaller particles have a higher electrical mobility; as a result, they are detected farther away from the center line. In the system, the left side shown in Fig. S1b represents positively charged particles, and the right side is for negatively charged particles. It should be noted that the particles that are passing through the middle of the detection spot in the AEMSA consist of not only the neutral particles but also larger charged particles if the charged particles have a low electrical mobility in the applied electric field that does change their positions away from the middle of the detection spot. Therefore, the main focus of this study is on the number of the positively and negatively charged particles, which can be affected by the electric field, and their ratios.

With a proper calibration process and operating condition, the AEMSA successfully provides information on particle electrical mobility and charge polarity. The details on the AEMSA calibration and operation were introduced in a previous work by Ahn and Chung (2010). They analyzed different-sized monodisperse particles classified by a DMA by using the AEMSA. The data showed a clear differentiation of charged particles, and the obtained charging fractions

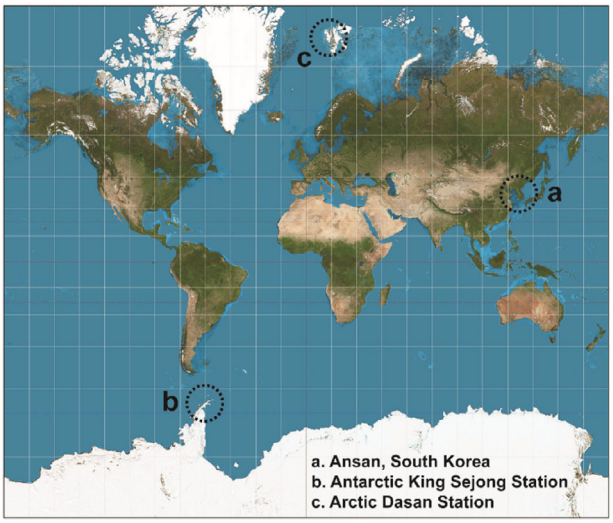

Fig. 1 – Locations for the aerosol electrical mobility spectrum analyzer (AEMSA) measurements: (a) Ansan in South Korea, (b) Antarctic King Sejong station, and (c) Arctic Dasan station (map of the world was retrieved from Wikipedia).

were consistent with the Fuchs modified empirical equation (Wiedensohler, 1988). In this study, the AEMSA was used to monitor charging fractions of atmospheric aerosols in the Antarctic King Sejong and Arctic Dasan stations. The results were compared with those obtained in a similar period in Ansan, South Korea, located in the midlatitude.

1.2. *Measurement sites and operating condition*

AEMSA measurements of bipolar charged particles were conducted in real time at three locations: Ansan, South Korea (37.3°N, 126.8°E), Antarctic King Sejong station (62°S, 58°W), and Arctic Dasan station (78°N, 11°E). The locations are indicated in Fig. 1, and the measurements were performed in March–May 2009. The Antarctic King Sejong station is located at Maxwell Bay, King George Island, in the South Shetland Islands. During the measurement period, the temperature at the location in March ranged from −5 to 5°C, and snow in the Antarctic melted. The Arctic Dasan station is located at the Ny-Ålesund International Science Village in Spitsbergen Island, Svalbard Archipelago, Norway. The temperature during the measurement period ranged from −10 to 5°C, and the land was completely covered by snow. All measurements were conducted in clear weather, and particle loss in the inlet port and other transportation lines in the AEMSA was minimized by using conducting materials. Furthermore, to prevent freezing and clogging issues resulting from the cold weather during the Antarctic and Arctic measurements, a warmer was installed to maintain the temperature around the AEMSA.

Concentrations of total, neutral (in fact, including larger charged particles not able to be classified by the electric field due to their lower electrical mobilities), positively charged, and negatively charged particles were obtained for each test. Owing to the finite dimension of the detection region, a particle size range for detection is determined according to a fixed voltage applied to the AEMSA. For example, if a particle placed in a very strong electric field has very high electrical mobility, the particle might be lost at the wall before reaching the detection region, where a CCD camera records the images of particles. Table 1 shows the operating condition of the AEMSA and size range for each case. Particles with sizes approximately from 10 to 300 nm were analyzed, and this corresponds to applied voltages from 80 to 3000 V. Each data point was obtained from 3-min measurement. The experiments in Ansan in South Korea, the Antarctic, and the Arctic were carried out around the same time, providing useful information for understanding different particle charge characteristics in the Antarctic and Arctic regions as well as midlatitudes, i.e., Ansan, South Korea.

Table 1 – Information on measurement locations and operating conditions of the aerosol electrical mobility spectrum analyzer (AEMSA)

Location	Date (mm/dd)	Voltage (V)	Size range (nm)
Ansan, South	04/07	300	20–80
Korea	04/08	3000	70–300
(37.3°N,	04/09	3000	70–300
126.8°E)	04/12	1500	47–220
Antarctic	03/10–03/11	300	20–80
King Sejong	03/12	600	30–120
station	03/13	3000	70–300
(62°S, 58°W)	03/14	80	11–40
Arctic Dasan	05/28–05/29	3000	70–300
station	05/29–05/30	1500	47–220
(78°N, 11°E)	05/30–05/31	300	20–80
	05/31–06/01	80	11–40

2. Results and discussion

2.1. *Ansan, South Korea*

Fig. 2 shows the concentration data on the atmospheric particles obtained in Ansan. The operating condition and corresponding analyzed particle size range are presented in Table 1. The left figures in Fig. 2 show the measured particle concentrations, and the right figures represent the ratio between positively and negatively charged particles (N(+)/N(–)). The red dashed line indicates the 1:1 line, i.e., the same proportion of positively and negatively charged particles. The x-axis represents the hours of the day. It is shown that the total concentrations change with time, and the trend of the charged-particle concentrations follows that of the total concentrations. In general, although there are some fluctuations, positively and negatively charged particles are fairly well-balanced, i.e., N(+)/N(–) is close to 1. However, from 6:00 pm on April 9, the population of negatively charged particles in the range of 70–300 nm started to exceed slightly that of the positively charged particles. The charging state of the same size range, i.e., 70–300 nm, was examined again on April 12. The trend of the concentration variation was different from that on April 9, having a peak concentration at approximately 1:00–2:00 pm. At this time, the negatively charged particles

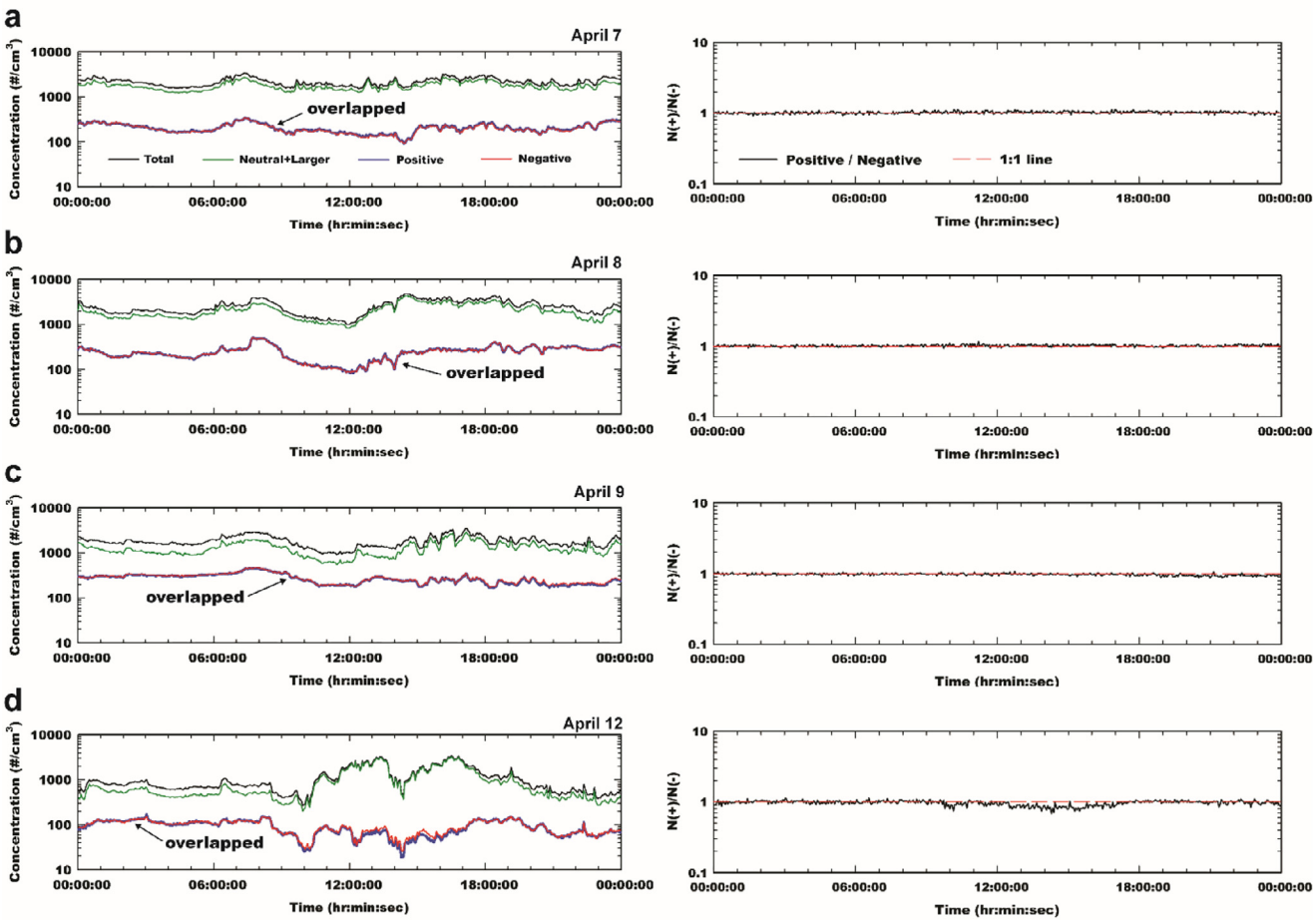

Fig. 2 – Particle concentrations measured by the AEMSA and the estimated charged-particle polarity ratio, N(+)/N(–), in Ansan, South Korea, on (a) April 7, (b) April 8, (c) April 9, and (d) April 12.

were more abundant by 20% than the positively charged particles. In addition, the shapes of concentration variation on April 7 (Tuesday), 8 (Wednesday), and 9 (Thursday) were very similar, showing relatively higher concentrations obtained at 7:00–8:00 am and later in the afternoon. This might have been caused by traffic during commuting hours, which may not be applicable to April 12 (Sunday). The well-balanced and stable charged-particle polarity ratio in urban environments is broadly in agreement with previous studies (Dos Santos et al., 2015; Hirsikko et al., 2007; Retalis and Retalis, 1998; Rohan Jayaratne et al., 2016). Hirsikko et al. (2007) found that concentrations of both positive and negative ions increased significantly near traffic-related sources where they assumed that the ions should be produced, which was revealed by the wind sector analysis. The ion concentration is closely associated with the particle charging. Therefore, we expect that by the abundant positive and negative ions in the urban environment, the charge polarity of atmospheric particles might tend to be well-balanced.

2.2. *Antarctic King Sejong station*

Atmospheric particle concentrations and charged-particle polarity ratios obtained at the Antarctic King Sejong station are shown in Fig. 3. Each day has a different trend in concentration variation. Fig. 3a shows that the concentrations varied significantly with time. In general, the trend of concentration variation for total particles was similar to that for the charged particles. However, at 4:00–5:30 pm and after 8:00 pm on March 10–11, although a variation in concentration of total particles was observed, the charged particles did not change significantly, or their concentrations even decreased. This means the charging rate was reduced. However, it seems that the different charging rates did not affect the polarity ratio of the charged particles significantly, which remained approximately 1.35 during the day. A pronounced tendency of the variations of concentration and polarity ratio could not be found in the Antarctic region or in the Arctic region. This might be related to the absence of artificial factors, such as industrial sources. A simultaneous chemical analysis of the particles might need to be performed to understand the trend more clearly.

The trends of the concentration variation on March 12 and 13 are very different. Relatively small peaks appeared several times during the measurement on March 12, but stable concentration variation was observed on March 13, except for a significant increase in charged-particle concentrations at approximately 9:00–10:00 am. However, the overall trends of the polarity ratio on March 12 and 13 were similar. In the

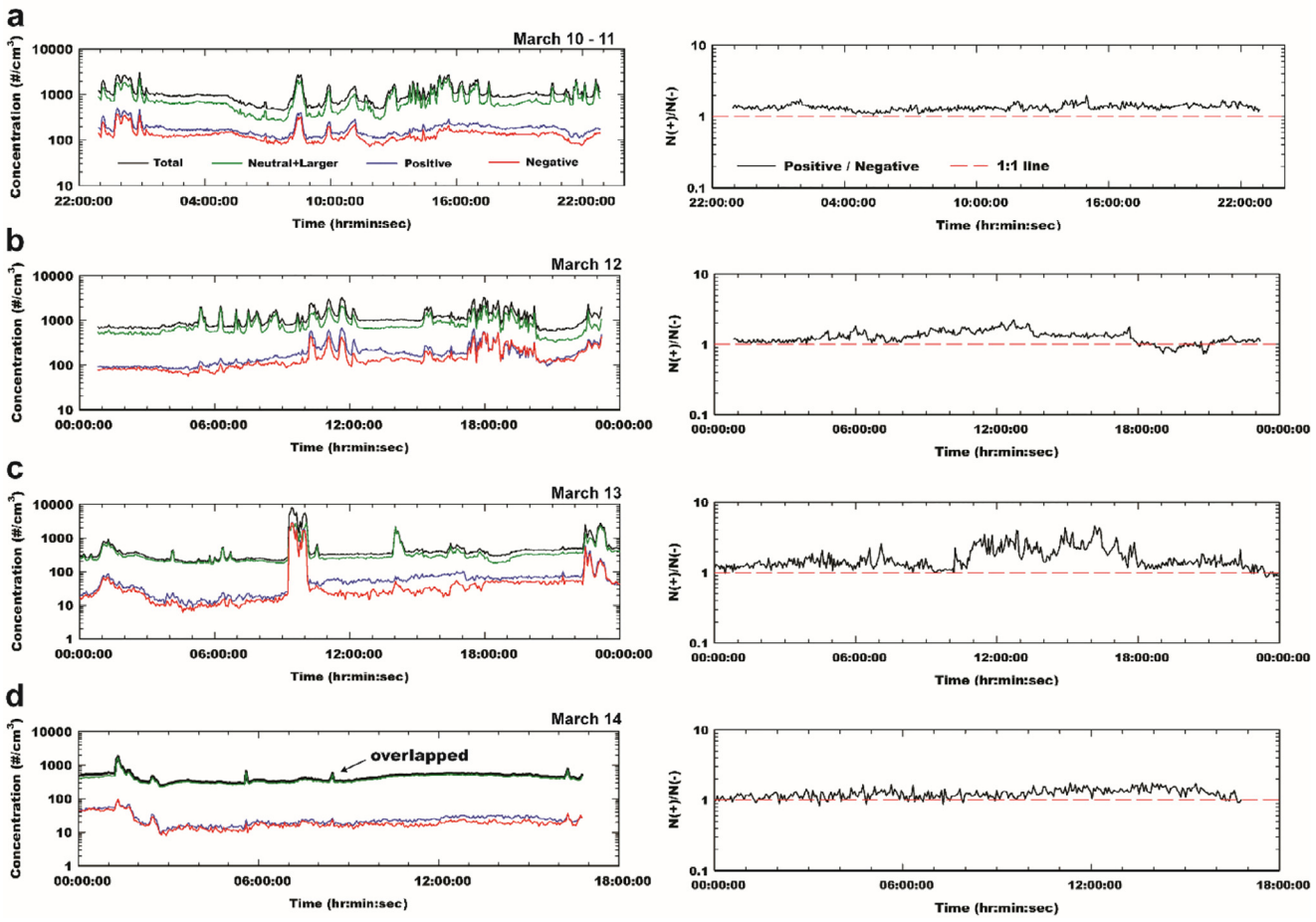

Fig. 3 – Particle concentrations measured by the AEMSA and the estimated charged-particle polarity ratio, N(+)/N(–), at the Antarctic King Sejong station on (a) March 10–11, (b) March 12, (c) March 13, and (d) March 14.

early morning, at 6:00–7:00 am, a gradual increase in positively charged particles was observed, following which, after the balance between the positively and negatively charged particles continued for a while, a significant increase in the positively charged particles was observed until 6:00 pm for both days. Interestingly, on March 13, the number of positively charged particles reached more than four times that of the negatively charged particles. Moreover, a pronounced difference in the polarity ratio before and after the concentration increase at 9:00–10:00 am was observed on March 13. It seems that the significant increase of the particle concentration triggered the imbalance of the charged particles. Without a significant variation in total concentration on March 14, slightly more positively charged particles were estimated.

2.3. *Arctic Dasan station*

Fig. 4 shows the data for the concentrations and charged-particle polarity ratios obtained at the Arctic Dasan station on May 28–June 1. Each measurement started at approximately 2:00 pm in the afternoon. In general, the concentrations varied irregularly, and a distinct routine could not be found easily. Measurements on May 29–30 and May 31–June 1 show a gradual decrease in total concentration without any specific event, and the concentration of the positively charged particles was steadily higher than for the negatively charged particles. The charged-particle polarity ratios for both cases were mostly above 1, approximately 3. On May 28–29 and May 30–31, the total concentrations fluctuated widely until 10:00–11:00 pm, following which the opposite trends were observed in the early morning, i.e., increasing (May 28–29) and decreasing (May 30–31) concentration. Furthermore, at the beginning of the measurement in the afternoon of both days, the charged-particle polarity ratio was close to or below 1. After 3:00 pm on May 30, the negatively charged particles exceeded the positively charged particles more than a factor of 10. However, throughout the measurements, the overall charged-particle polarity ratio was high and varied significantly. During the measurements, the Arctic region was in the period of the midnight sun. Therefore, the much higher and steady concentrations of the positively charged particles might be related to the effect of continuous influx of sun radiation at the measurement site.

2.4. *Charged-particle polarity ratio*

The difference in the obtained charged-particle polarity ratios for the different locations is evident in Fig. 5a. In Ansan, South Korea, located in the midlatitude, the numbers of the

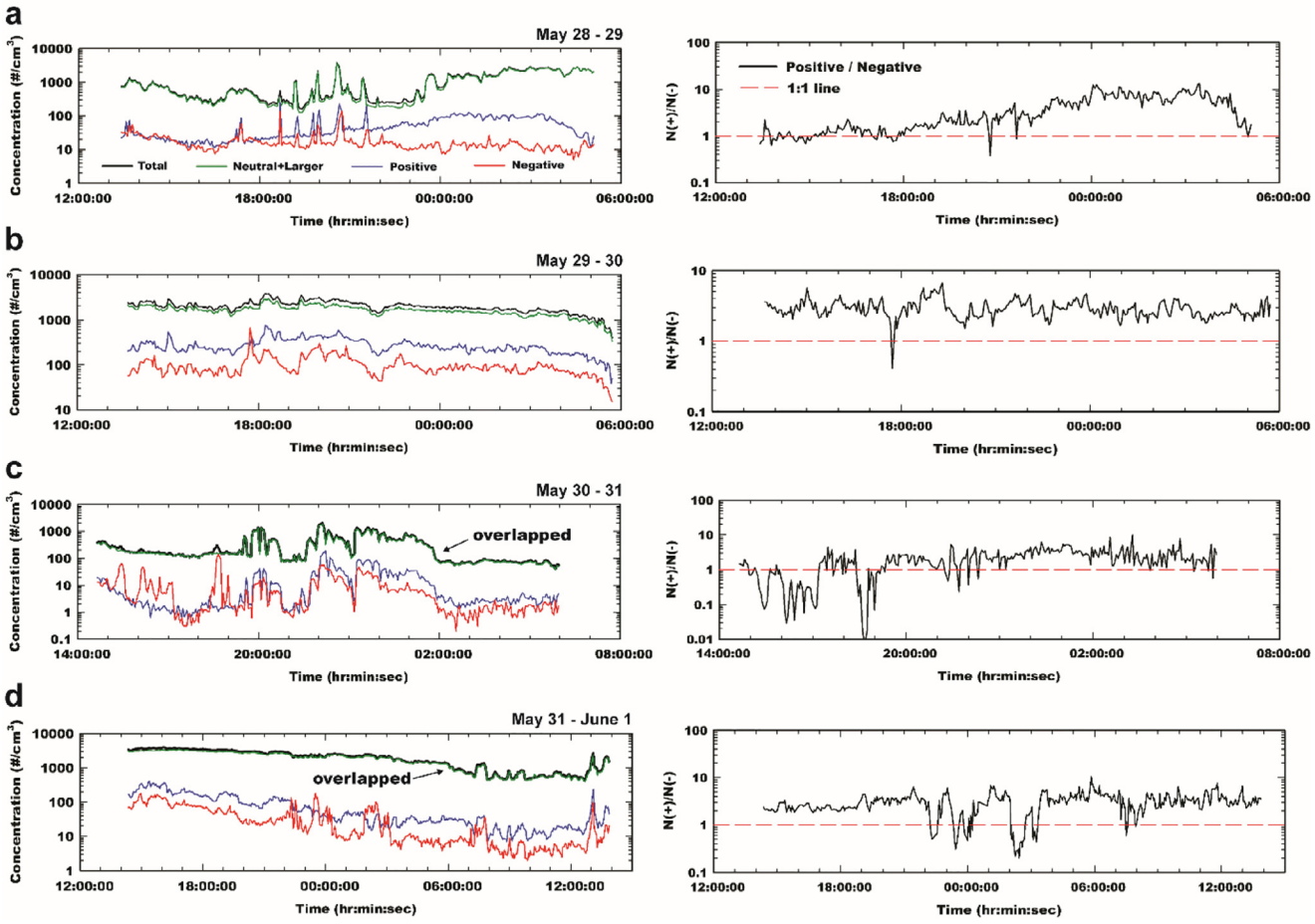

Fig. 4 – Particle concentrations measured using the AEMSA and the estimated charged-particle polarity ratio, N(+)/N(–), at the Arctic Dasan station on (a) May 28–29, (b) May 29–30, (c) May 30–31, and (d) May 31–June 1.

positively and negatively charged particles were fairly well balanced. Compared with this, the Antarctic and Arctic areas showed 1.4 and 2.8 times higher positively charged-particle concentrations than negatively charged ones, respectively. Furthermore, the charged-particle polarity ratio is shown according to particle size range in Fig. 5b. When operating the AEMSA with applied voltages of 300 and 3000 V, the analyzed particle size ranges were 20–80 and 70–300 nm, respectively. It was revealed that, for the larger particle size range, i.e., 70–300 nm, a higher ratio between positively and negatively charged particles was obtained in the Antarctic and Arctic regions than that of the smaller particles. This might be because, as particle size increases, the particles carry charges more easily. Moreover, owing to the proportional relationship between surface area and charges on particles, larger particles are more likely to carry positive charges (Yair and Levin, 1989).

The results of the charged-particle concentration according to time were also plotted in Fig. 6, i.e., 00:00–06:00, 06:00–12:00, 12:00–18:00, and 18:00–24:00. Fig. 6a clearly shows that, in South Korea, the numbers of the positively and negatively charged particles were similar, regardless of time. Meanwhile, the Antarctic and Arctic data spread out and are weighted toward the positively charged particles. Specifically, in the Antarctic measurement data at 6:00 am to 6:00 pm in Fig. 6b (red and gray colored symbols), the number of positively charged particles exceeded that of the negatively charged particles considerably. In the Arctic region (Fig. 6c), a large number of negatively charged particles were observed sometimes, but, in general, considerably more positively charged particles were present at all times.

There might be several reasons for the presented results, showing distinctive and different charge characteristics in South Korea and the Antarctic and Arctic regions. Therefore, possible explanations are listed below.

(1) The different latitudes of South Korea and the Antarctic and Arctic regions might alter the charge characteristics. Cosmic rays play an important role in determining electrical properties of the atmosphere (Carslaw et al., 2002; Usoskin and Kovaltsov, 2006). Cosmic rays consist of high-energy protons, atomic nuclei, and electrons, and much of the cosmic-ray content is hydrogen nuclei, approximately 90% of total nuclei. Some of these cosmic rays are deflected to the North and South Poles because of the Earth's magnetic field. This might result in the different charge characteristics at the poles and other parts of the Earth.
(2) During the measurements in the Arctic, the fields were covered by snow, which may influence the terrestrial compo-

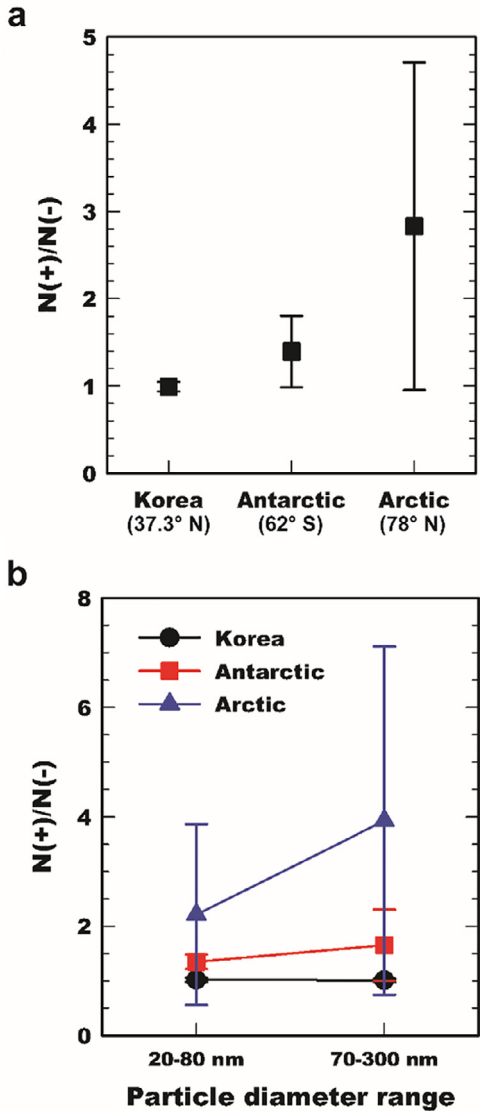

Fig. 5 – Charged-particle polarity ratio obtained for different (a) locations and (b) particle size ranges.

nent of natural radiation. Moreover, it has been revealed that negative charging of ice occurs during evaporation (Dong et al., 1994; Dong and Hallett, 1992). This may be one of the possible factors for reducing positively charged particles in the atmosphere over the Antarctic area, where snow was melting during the measurement period.

(3) During the measurement period in the Arctic area, solar activity continued for 24 hr a day owing to the midnight sun. This unique solar activity of continuous inflow of solar radiation may result in different consequences for the charge characteristics of the atmospheric particles compared with the cases for Ansan and the Antarctic area.

3. Conclusions

The charging states of atmospheric particles in the Antarctic and Arctic regions were investigated by using the AEMSA,

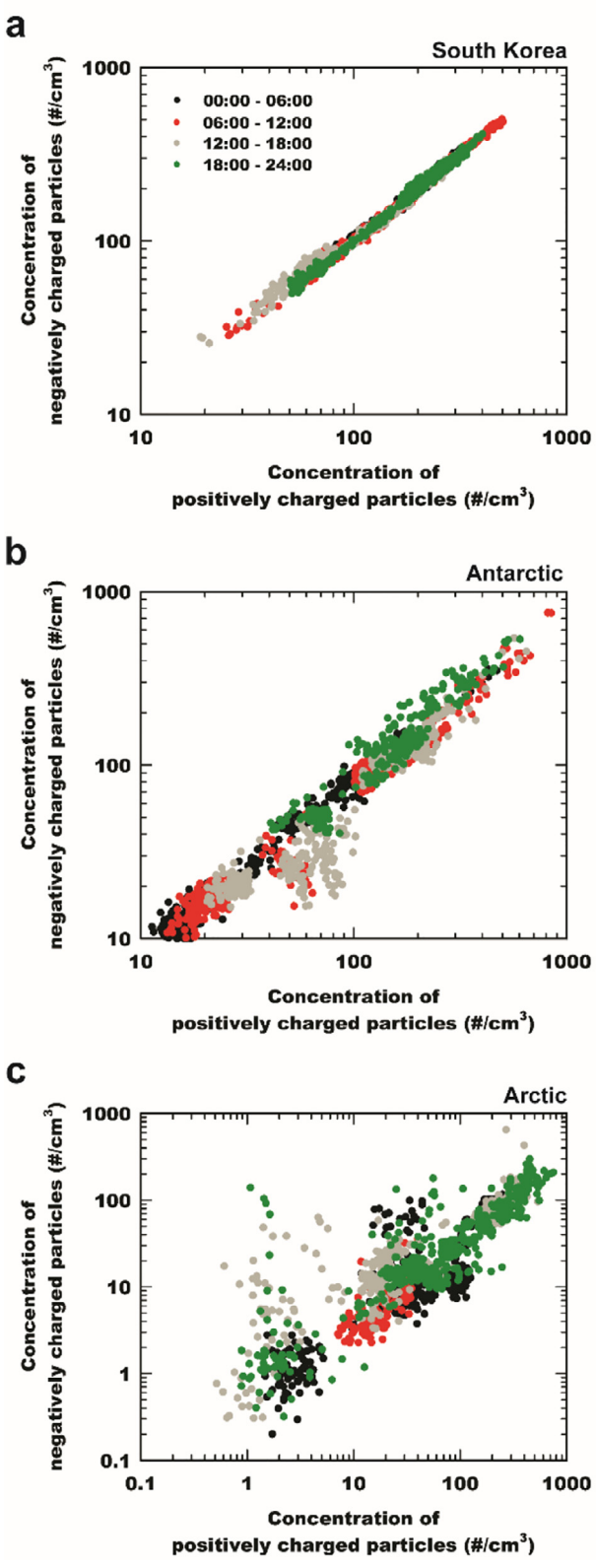

Fig. 6 – Concentrations of positively and negatively charged particles estimated in specific time ranges at (a) Ansan, South Korea, (b) Antarctic region, and (c) Arctic region.

which is an instrument for monitoring aerosol electrical mobility and charge at a fixed applied voltage. The AEMSA was developed at Hanyang University in South Korea. The experiments were performed at the Antarctic King Sejong and Arctic Dasan stations, and the results were compared with the particle-charging state measured in Ansan, South Korea. Charged-particle polarity ratios measured in Ansan revealed that the numbers of positively and negatively charged particles were well balanced, resulting in approximately zero net charge. However, positively charged particles exceeded the negatively charged particles greatly in both the Antarctic and the Arctic regions. The gap between those particles are larger in the Arctic and followed by the Antarctic. The charging state for atmospheric aerosols plays an important role in climate change. Therefore, the developed AEMSA system and the findings in this study can provide a useful source for research related to particle charge characteristics such as cloud formation mechanisms.

Declaration of competing interest

The authors declare that they have no known competing financial interests or personal relationships that could have appeared to influence the work reported in this paper.

Acknowledgments

This work was supported by the research fund of Hanyang University (HY-2019-P).

Appendix A. Supplementary data

Supplementary material associated with this article can be found in the online version at doi:10.1016/j.jes.2020.12.028.

REFERENCES

Ahn, K.H., Chung, H., 2010. Aerosol electrical mobility spectrum analyzer. J. Aerosol Sci. 41, 344–351.
Carslaw, K.S., Harrison, R.G., Kirkby, J., 2002. Cosmic rays, clouds and climate. Science 298, 1732–1737.
Charlson, R.J., Schwartz, S.E., Hales, J.M., Cess, R.D., Coakley Jr., J.A., Hansen, J.E., et al., 1992. Climate forcing by anthropogenic aerosols. Science 255, 423–430.
Chu, B., Liu, Y., Ma, Q., Ma, J., He, H., Wang, G., et al., 2016. Distinct potential aerosol masses under different scenarios of transport at a suburban site of Beijing. J. Environ. Sci. 39, 52–61.
Dallósto, M., Beddows, D.C.S., Tunved, P., Krejci, R., Ström, J., Hansson, H.C., et al., 2017. Arctic sea ice melt leads to atmospheric new particle formation. Sci. Rep. 7, 1–10.
Dong, Y., Hallett, J., 1992. Charge separation by ice and water drops during growth and evaporation. J. Geophys. Res. 97, 361–371.
Dong, Y., Oraltay, R.G., Hallett, J., 1994. Ice particle generation during evaporation. Atmos. Res. 32, 45–53.
Dos Santos, V.N., Herrmann, E., Manninen, H.E., Hussein, T., Hakala, J., Nieminen, T., et al., 2015. Variability of air ion concentrations in urban Paris. Atmos. Chem. Phys. 15, 13717–13737.
Gilbert, J.S., Lane, S.J., Sparks, R.S.J., Koyaguchi, T., 1991. Charge measurements on particle fallout from a volcanic plume. Nature 349, 598–600.
Han, Y., Fang, X., Zhao, T., Kang, S., 2008. Long range trans-Pacific transport and deposition of Asian dust aerosols. J. Environ. Sci. 20, 424–428.
Hansen, J., Sato, M., Ruedy, R., 1997. Radiative forcing and climate response. J. Geophys. Res. 102, 6831–6864.
Harrison, R.G., 2004. The global atmospheric electrical circuit and climate. Surv. Geophys. 25, 441–484.
Harrison, R.G., Nicoll, K.A., Ulanowski, Z., Mather, T.A., 2010. Self-charging of the Eyjafjallajökull volcanic ash plume. Environ. Res. Lett. 5, 024004.
He, Y., Gu, Z., Lu, W., Zhang, L., Okuda, T., Fujioka, K., et al., 2019. Atmospheric humidity and particle charging state on agglomeration of aerosol particles. Atmos. Environ. 197, 141–149.
Hirsikko, A., Yli-Juuti, T., Nieminen, T., Vartiainen, E., Laakso, L., Hussein, T., et al., 2007. Indoor and outdoor air ions and aerosol particles in the urban atmosphere of Helsinki: characteristics, sources and formation. Boreal Environ. Res. 12, 295–310.
Jokinen, T., Sipilä, M., Kontkanen, J., Vakkari, V., Tisler, P., Duplissy, E.M., et al., 2018. Ion-induced sulfuric acid–ammonia nucleation drives particle formation in coastal Antarctica. Sci. Adv. 4, 1–7.
Kumar, R., Guleria, R.P., 2017. A review of potential radiative effect of aerosol on climate. Indian J. Radio Space Phys. 46, 5–14.
Lee, H.K., Ahn, K.H., 2017. Charging effect on the 80–200 nm size atmospheric aerosols during a lightning event. Aerosol Air Qual. Res. 17, 2624–2630.
Li, Y., Zhang, H., Zhang, Q., Xu, Y., Nadykto, A.B., 2020. Interactions of sulfuric acid with common atmospheric bases and organic acids: thermodynamics and implications to new particle formation. J. Environ. Sci. 95, 130–140.
Liu, Z., Sun, Y., Zhang, Y., Qin, S., Sun, Y., Mao, H., et al., 2020. Desert soil sequesters atmospheric CO_2 by microbial mineral formation. Geoderma 361, 114104.
McMurry, P.H., 2000. A review of atmospheric aerosol measurements. Atmos. Environ. 34, 1959–1999.
Nicoll, K.A., Harrison, R.G., Ulanowski, Z., 2011. Observations of Saharan dust layer electrification. Environ. Res. Lett. 6, 1–8.
Raes, F., Janssens, A., 1985. Ion-induced aerosol formation in a H_2O-H_2SO_4 system-I. Extension of the classical theory and search for experimental evidence. J. Aerosol Sci. 16, 217–227.
Renard, J.B., Tripathi, S.N., Michael, M., Rawal, A., Berthet, G., Fullekrug, M., et al., 2013. In situ detection of electrified aerosols in the upper troposphere and stratosphere. Atmos. Chem. Phys. 13, 11187–11194.
Retalis, D., Retalis, A., 1998. Effects of air pollution and wind on the large-ion concentration in the air above Athens. J. Geophys. Res. Atmos. 103, 13927–13932.
Rohan Jayaratne, E., Ling, X., Morawska, L., 2016. Charging state of aerosols during particle formation events in an urban environment and its implications for ion-induced nucleation. Aerosol Air Qual. Res. 16, 348–360.
Rycroft, M.J., Odzimek, A., Arnold, N.F., Füllekrug, M., Kułak, A., Neubert, T., 2007. New model simulations of the global atmospheric electric circuit driven by thunderstorms and electrified shower clouds: the roles of lightning and sprites. J. Atmos. Solar-Terrestrial Phys. 69, 2485–2509.
Saunders, 1992. A review of thunderstorm electrification processes. J. Appl. Meteorol. 32, 642–655.
Snow-Kropla, E.J., Pierce, J.R., Westervelt, D.M., Trivitayanurak, W., 2011. Cosmic rays, aerosol formation and cloud-condensation nuclei: sensitivities to model uncertainties. Atmos. Chem. Phys. Discuss. 11, 2697–2732.

Usoskin, I.G., Kovaltsov, G.A., 2006. Cosmic ray induced ionization in the atmosphere: full modeling and practical applications. J. Geophys. Res. Atmos. 111, 1–9.
Wiedensohler, A., 1988. An approximation of the bipolar charge distribution for particles in the submicron size range. J. Aerosol Sci. 19, 387–389.
Yair, Y., Levin, Z., 1989. Charging of polydispersed aerosol particles by attachment of atmospheric ions. J. Geophys. Res. 94, 13085–13091.
Yu, F., Turco, R.P., 2001. From molecular clusters to nanoparticles: role of ambient ionization in tropospheric aerosol formation. J. Geophys. Res. Atmos. 106, 4797–4814.